The Journal of Experimental Biology 208, 2783-2798
Published by The Company of Biologists 2005
doi:10.1242/jeb.01680

V-ATPase expression during development of *Artemia franciscana* embryos: potential role for proton gradients in anoxia signaling

Joseph A. Covi* and Steven C. Hand

Division of Cellular, Developmental and Integrative Biology, Department of Biological Science, Louisiana State University, Baton Rouge, LA 70803, USA

*Author for correspondence (e-mail: jcovi1@lsu.edu)

Accepted 11 May 2005

Summary

Under anoxia, *Artemia franciscana* embryos downregulate metabolic processes and approach an ametabolic state. Entrance into this quiescent state is accompanied by a profound acidification of the intracellular space, and more than two decades of research now clearly demonstrates that this acidification is critical to metabolic downregulation in anoxic embryos. However, the proximal mechanisms responsible for the pH shift remain largely unidentified. Here, we report evidence demonstrating expression of the V-ATPase in encysted embryos and present an argument for its involvement in the intracellular acidification induced by anoxia. We identified a single B-subunit cDNA sharing the greatest degree of sequence similarity with 'generalist-type' homologues from mammals (brain-type) and invertebrates. Quantitative analysis of B-subunit mRNA demonstrates differential expression throughout early development, and western blot analyses confirm the expression of at least six V-ATPase subunits in both heavy membranes and microsomal vesicles. The critical need for proton pumping during the anoxia-tolerant stage of development is demonstrated by incubation with the V-ATPase inhibitor bafilomycin A_1, which halts embryonic development. Importantly, net proton flux from V-ATPase-acidified compartments to the surrounding cytoplasm is likely under anoxia and may significantly contribute to the enigmatic acidification critical to quiescence.

Key words: V-type ATPase, mRNA expression, protein expression, quiescence, diapause, brine shrimp, B-subunit cDNA, acidification, bafilomycin, oligomycin, hatching success.

Introduction

When released *en masse* in the autumn, encysted embryos of the brine shrimp, *Artemia franciscana*, can encounter prolonged bouts of anoxia when buried in anoxic sediments, algal mats and windrows of other embryos along the shore (Clegg, 1974). Not surprisingly, these embryos possess a profound mechanism of ensuring long-term survivorship in a hydrated anoxic state. Exposure to anoxia induces one of the most dramatic intracellular acidifications ever recorded for a eukaryotic organism (>1.6 pH units; Busa et al., 1982), and more than two decades of research has convincingly demonstrated that this event is one of the primary effectors of a potentially complete metabolic shutdown (for related reviews, see Clegg, 2001; Guppy and Withers, 1999; Hand, 1997; Hand and Hardewig, 1996; Hochachka and Guppy, 1987; Storey and Storey, 1990). However, while a great deal of progress has been made in describing the role of acidification in metabolic depression (e.g. Hand, 1997, 1998; Hand et al., 2001), very little is yet known about the proximal mechanisms responsible for the decrease in intracellular pH (pH_i) itself. By pushing the limits of assumptions about physiologically relevant variables impacting pH_i, a maximum of 72% of the proton equivalents required for the observed acidification could be explained (Kwast et al., 1995). More conservative estimates suggest that the explainable acidification may be as low 20–26% (Busa and Nuccitelli, 1984; Kwast et al., 1995). Importantly, the release of protons from membrane-bound acidic compartments is not considered in these analyses, while just such a phenomenon has been shown to cause significant acidification of the surrounding cytoplasm in cultured Hep 2 cells during osmotic swelling of organelles (Madshus et al., 1987). It is plausible that a coordinated release of protons from acidic compartments within encysted *Artemia* embryos could also produce a significant drop in pH_i. If this is the case, one might predict that such compartments would be acidified during aerobic development by a proton pumping system, such as the ATP-dependent V-type proton pump (V-ATPase). In the present study, we provide evidence demonstrating that the V-ATPase is expressed in *A. franciscana* throughout development of the encysted embryonic stage. An analysis of the subcellular distribution of V-ATPase subunits, in the context of recent literature, suggests expression in membranes of intracellular compartments likely to possess an acidic lumen. Importantly, the release of protons from these compartments, upon anoxic

exposure, could help facilitate a metabolic downregulation essential to the long-term survival of encysted *A. franciscana* embryos.

It is important to note that the ability of this free-floating gastrula to downregulate metabolism in response to anoxia (Hand and Gnaiger, 1988) is present from the moment development begins, but is subsequently lost when they emerge from their protective cyst coat after 8–12 h of aerobic development (Ewing and Clegg, 1969; Stocco et al., 1972). The encompassing cyst coat, restricted to the embryonic stage, isolates the embryo from its environment with a highly selective permeability barrier (for discussion, see Trotman, 1991). This barrier precludes the involvement of exogenous H^+ equivalents in the previously discussed acidification (Busa et al., 1982). Unfortunately, the nature of the cyst shell confounds examination of the proton-generating mechanisms responsible for the pH transition by preventing the direct measurement of pH_i *in vivo* with the use of microelectrodes or reporter compounds. For this reason, ^{31}P-NMR is the only method to yet provide *in vivo* measurements of embryonic pH_i (Busa et al., 1982; Busa and Nuccitelli, 1984; Clegg et al., 1995; Kwast et al., 1995), although a limitation inherent in this method suggests that acidic compartments may be involved in anoxia signaling.

While the caveats of using ^{31}P-NMR to determine *in vivo* pH_i have been covered elsewhere (Busa et al., 1982), it is important to note here that the technique is limited by its dependence on the presence of free inorganic phosphate (P_i) in the compartment(s) being observed. Consequently, compartments having low P_i concentration or low relative volume have a negligible effect on the average pH being measured for a population of whole embryos. In other words, protons stored in these compartments would remain undetected until their release into a space having a relatively high P_i content, whereupon the event would be observed as an acidification. One potentially undetected compartment might be the extracellular space, which has been noted in some organisms to contain as little as 20% of the P_i found in the cytoplasm (Grabe and Oster, 2001). Alternatively, undetected acidic compartments may be subcellular in nature, and their visualization precluded by the fact that they only contain a small percentage of free embryonic P_i. These presumably would include Golgi, tubules, exocytotic vesicles, coated vesicles, early and late endosomes, and lysosomes, all of which are likely to have functional roles during such events as production of the embryonic cuticle (cf. Criel, 1991), formation of yolk platelets (Giorgi et al., 1999; Warner et al., 2002) and yolk degradation (Komazaki and Hiruma, 1999; Perona et al., 1988; Perona and Vallejo, 1985, 1989). Indeed, membrane-bound yolk platelets themselves should be considered, as they are acidified to varying degrees for both maintenance and degradation in other species (Abreu et al., 2004; Fagotto, 1995; Fausto et al., 2001) and contain very little P_i in *A. franciscana* (Warner and Huang, 1979). An interesting commonality among all of these compartments is that their final luminal pH is set in part by the V-ATPase proton pump (Futai et al., 1998; Grabe and Oster, 2001; Nishi and Forgac, 2002), and thus this enzyme became the focal point of our research.

The V-ATPase is a multimeric complex composed of two primary domains (V_1 and V_0). The extra-membrane V_1 domain is comprised of eight different subunits, labeled A–H, and is responsible for ATP hydrolysis (Wieczorek et al., 2000). The membrane-spanning V_0 domain consists of at least three different subunits, labeled a, d and c, and is responsible for providing a proton path across the membrane (Forgac, 1998). When combined, these two domains form a molecular motor well known for both its broad distribution and diverse functional capacity for proton transport. For example, in addition to their role in acidification of intracellular compartments (Forgac, 2000; Futai et al., 2000), V-ATPases are also known to power acid secretion and secondary active transport in animal plasma membranes (for recent reviews, see Kawasaki-Nishi et al., 2003; Nelson and Harvey, 1999; Nelson et al., 2000; Wieczorek et al., 2000). Taking these facts into consideration, the V-ATPase is a prime candidate for facilitating the proton transport required to establish intracellular and/or extracellular acidic compartments in *A. franciscana* embryos.

We hypothesize that, in the face of severe energetic constraints imposed by anoxia, H^+ gradients between acidic compartments and the surrounding cytoplasm dissipate, producing an acidification critical to metabolic downregulation in *A. franciscana* embryos. As first steps in addressing this hypothesis, we examined expression of the V-ATPase during the early development of these embryos and demonstrate that *in vivo* inhibition of this proton pump by bafilomycin blocks normoxic development.

Materials and methods

Animals

Encysted embryos of the brine shrimp, *Artemia franciscana* Kellog (Great Salt Lake population), were either obtained in the dehydrated state (post-diapause) from Sanders Brine Shrimp Co. (Ogden, UT, USA) in 1999 or collected from the surface of the Great Salt Lake in the hydrated state (diapause) in September 2001. Diapause embryos were stored in plastic bottles containing 35‰ artificial seawater (Instant Ocean; Aquarium Systems, Eastlake, OH, USA) supplemented with NaCl to a final concentration of 60‰, protected from light exposure and maintained at 22–23°C. Embryo viability and preservation of the diapause state during storage were evaluated using published protocols (Reynolds and Hand, 2004). Post-diapause embryos were stored dry at –20°C and hydrated overnight at 0°C in 0.25 mol l^{-1} NaCl prior to experimental incubation. Staging of embryos was conducted using the same criteria described by Conte et al. (1977).

*Manduca sext*a were obtained as 3rd-instar larvae from a colony at the Arizona Research Labs Division of Neurobiology, University of Arizona (Willis and Arbas, 1998).

Dissections were performed according to Harvey et al. (1990) after larvae developed to the feeding phase of the 4th-instar stage.

Molecular cloning and sequencing of cDNA for subunit B of the V-ATPase

AMV reverse transcriptase (Promega, Madison, WI, USA) and a d18TV primer were employed to reverse transcribe poly(A+) mRNA from DNase-treated total RNA, previously isolated from 6 h aerobic *A. franciscana* embryos (Hardewig et al., 1996). A central domain of the V-ATPase B-subunit was amplified using degenerate primers (HATF2, HATR4; Weihrauch et al., 2001; Table 1). Following agarose gel purification, the amplified cDNA was cloned, and the insert was sequenced directly from the plasmid construct. After the identity of the cDNA fragment was confirmed by BLAST search of the GenBank database, the 3′ and 5′ ends were amplified by rapid amplification of cDNA ends (RACE) using a First Choice RLM RACE kit (Ambion, Austin, TX, USA) according to the manufacturer's instructions. The 5′ end was amplified from total RNA isolated from post-diapause embryos immediately after hydration (hour 0). Since amplification of the 3′ end is more efficient when mRNA is used, the 3′ end was amplified from mRNA previously isolated from diapause embryos. It is important to note that, because diapause embryos are developmentally arrested, the mRNA of these embryos is theoretically equivalent to that of post-diapause embryos before development is resumed (hour 0). RACE PCR products were gel purified, cloned and sequenced directly from the plasmid construct using specific primers designed with the assistance of Primer3 software (Rozen and Skaletsky, 2000). Sequencing utilized BigDye terminator chemistry and an ABI PRISM 3100 Genetic Analyzer (Applied Biosystems, Foster City, CA, USA). Sequences were assembled using Sequencher software (Gene Codes Co., Ann Arbor, MI, USA). An open reading frame (ORF) was identified using a freely available ORF tool available from The National Center for Biotechnology Information (http://www.ncbi.nlm.nih.gov). DNA-to-protein translation, pI estimation and theoretical calculation of relative molecular mass (M_r) were achieved using tools made available by the Swiss Institute of Bioinformatics (http://us.expasy.org/tools). Multiple sequence alignments were produced with Clustal X version 1.83 (Thompson et al., 1997). Sequences were annotated with GeneDoc version 2.6.002 (http://www.psc.edu/biomed/genedoc). Phylogenetic analysis was conducted with MEGA version 2.1 (Kumar et al., 2004). Based on the work of Hillis and Bull (1993), all bootstrap proportions $\geqslant$70% were considered strong support for a given clade.

Isolation of total RNA

RNase-free conditions were maintained throughout all isolations using published methods (Hardewig et al., 1996). Encysted embryos were washed using a modified dechorionation protocol (Kwast and Hand, 1993). All wash solutions were maintained at 0°C to prevent premature development and complete removal of the chorion. Aseptic embryos were then incubated at 22–23°C with shaking at 110 r.p.m. in Erlenmeyer flasks containing 35‰ artificial seawater.

Two different procedures were employed for isolating total RNA. In the first case, hydrated embryos were kept on ice until the start of incubation, and starting times were staggered, allowing all time points to be processed within 20 min of each other. Developing embryos were equilibrated with a 40:60 O_2:N_2 gas mixture (cf. Carpenter and Hand, 1986), and triplicate extractions were performed for each time point by homogenization in a guanidinium thiocyanate-based buffer, followed by isolation of total RNA by centrifugation through a CsCl cushion as described by Hardewig et al. (1996). Alternatively, incubation of hydrated embryos was initiated synchronously, and development proceeded in a medium equilibrated with room air. At predetermined intervals, triplicate flasks of embryos were suspended in ice-cold 35‰ artificial seawater to arrest development until homogenization. For each time point, embryos were filtered, rinsed with cold DEPC water and blotted dry. RNA extractions were performed

Table 1. *Oligonucleotide primers for cloning, sequencing and expressing* A. franciscana *V-ATPase B-subunit*

Primer title	Primer sequence (5′→3′)	Position in cDNA	Use
HATR4	Degenerate (Weihrauch et al., 2001)	719–739	A, S
HATF2	Degenerate (Weihrauch et al., 2001)	1092–1110	A, S
5′ RACE inner	GAACCGAGCAGTTTCCATATTC	731–752	R, S
5′ RACE outer#2	GATCCATTTCTGCCTTCAACTC	1041–1062	R, S
3′ RACE inner	CTACGAAAGAGCTGGCAGAGTT	1024–1045	R, S
3′ RACE outer	AGTGTGAGAAACATGTGCTCGT	885–906	R, S
Bsub3′walk	GTAGGCGAAGAAGCTCTTAC	1337–1356	S
Bsub3′walk2	TTGGATGGCAACTTCTTCGT	1458–1477	S
5′walkback	TGCTGGTCTTCCTCACAAT	601–622	S
5′walk1	GGACCATTGACTCCAGAAACA	166–186	S
expr(L)Bsub2	CTGGGAATTCGTGAATATGGAAACT	728–742	E, S
expr(R)Bsub2	TGCCTCGAGTAGTAATGTCATCGTT	1094–1108	E, S

Adapter sequences containing restriction sites are underlined. Abbreviations: A, primer used in first PCR amplification; R, primer used in RACE amplification; S, primer used in sequencing cDNA; E, primer used for amplification of sequence employed in protein expression.

with an RNeasy Midi kit (Qiagen, Valencia, CA, USA) as per the manufacturer's instructions for animal tissues. In brief, 0.91 g of embryos were homogenized in 12 ml of chaotropic buffer, and RNA was isolated *via* selective binding to a silica-gel-based membrane (Qiagen). For the hour 24 samples, swimming nauplii were separated from the shed chorion using a Buchner funnel. To prevent overloading of the membrane, only 0.76 g of nauplii were used for each replicate. This reduced mass compensated for the loss of the inert embryonic chorion during hatching. As an internal control, 1 μg of synthetic RNA for strawberry chitinase was added to the chaotropic buffer prior to each homogenization (see below for details). Homogenates were centrifuged at 12 000 ***g*** for 10 min at 0°C to remove cell debris, and 10 ml of the resultant supernatant was applied to the RNeasy spin membrane. The same procedure was used to isolate RNA from diapause embryos. Diapause mRNA used for RLM-RACE was isolated using this total RNA and an Oligotex mRNA Mini kit (Qiagen).

The concentration of RNA in each sample was determined spectrophotometrically (A260). Purity of the RNA preparations was determined by spectrophotometric scan (250–350 nm) of each sample. DNA contamination was determined by percent loss after treatment with Rnase-free DNase (RQ1; Promega) followed by acidic PCIA (phenol: chloroform: isoamyl alcohol) extraction and ethanol precipitation. Integrity of the RNA was examined by both northern blot analyses and ethidium bromide staining of 18 and 28 S ribosomal RNA bands on a denaturing agarose gel.

Production of synthetic RNA for northern controls and dot blot standards

A genomic DNA clone of chitinase II from strawberry (Khan, 2002) was used for the production of synthetic RNA to be used as an internal control for the *A. franciscana* total RNA isolation. The clone consisted of 1002 base pairs of genomic DNA ligated into a pGEM-T easy vector (Promega, Madison, WI, USA) that had been digested with *Eco*RI. This plasmid construct was linearized using *Pst*I (Gibco-BRL, Gaithersburg, MD, USA) and subjected to proteinase K digestion, phenol:CIA extraction and ethanol precipitation. A MEGAscript *in vitro* transcription kit (Ambion) was used to transcribe synthetic RNA with T7 polymerase. After treatment with DNase I, the synthetic RNA was precipitated with lithium chloride and stored as a precipitate at –80°C.

The same procedure was used to produce synthetic RNA from the *A. franciscana* V-ATPase B-subunit clone, originally amplified with degenerate primers. In this case, however, the plasmid construct was digested with *Spe*I (Gibco-BRL) prior to *in vitro* transcription, and the synthetic RNA was used as a positive control for the oligonucleotide probing of northern blots.

Northern and dot blots

Total RNA samples (5 μg) were dried in a Savant speedvac (Farmingdale, NY, USA), heat denatured at 55°C for 15 min in 12 μl of denaturing buffer (80% deionized formamide, 3.7% v/v formaldehyde and 1× MOPS running buffer, pH 7.0), quick cooled in an ice slurry, and electrophoresed on a 1.2% agarose gel containing 1× MOPS (pH 7.0) and 37% v/v formaldehyde. Gels were rinsed in several washes of DEPC-treated water to remove formaldehyde. RNA was transferred to a nylon membrane (Genescreen Plus; Dupont, NEN, Boston, MA, USA) over a period of 17 h by capillary action using 10× SSPE buffer (0.1 mol l^{-1} Na_2HPO_4/NaH_2PO_4 pH 7.0, 1.8 mol l^{-1} NaCl and 10 mmol l^{-1} EDTA). After transfer, membranes were rinsed with 5× SSPE, dried for 1 h at 60°C, and the RNA was UV crosslinked to the membrane. Crosslinked blots were washed in hybridization buffer (5× SSPE, 2% SDS, 10 μg ml^{-1} Rnase-free calf thymus DNA and 50 μg ml^{-1} yeast RNA), pre-hybridized in the same buffer for 6 h at 65°C, and hybridized with a ^{32}P-dCTP (NEN-PerkinElmer, Boston, MA, USA)-labeled cDNA probe (see below) for 50 h at 65°C. The membranes were subsequently washed twice in 2× SSPE with 0.1% SDS, followed by a single wash in 0.2× SSPE with 0.1% SDS. The final blots were then wrapped in cellophane and exposed to a phosphor screen. Imaging was conducted with either a STORM 840 phosphor imager or a Typhoon 8600 variable mode imager from Molecular Dynamics (Sunnyvale, CA, USA).

To quantify the strawberry synthetic RNA in *A. franciscana* samples after isolation, 5 μg aliquot samples of total RNA were subjected to dot blot analysis. Procedures followed a published protocol (Hardewig et al., 1996) with slight modification. All samples were combined with 85.8 μl of denaturing reagent (80% deionized formamide, 3.7% formaldehyde and 2× SSPE, pH 7.0) and 5 μg of yeast RNA, diluted to a final volume of 100 μl and heat denatured at 55°C for 15 min. No loading dye was used. After the samples were applied to the membrane, sample wells were rinsed with 300 μl of 2× SSPE. The membrane was then dried for 30 min at 70°C before UV crosslinking. The hybridization procedure followed that outlined for northern blots.

Northern and dot blot probes were labeled using a published protocol (Hardewig et al., 1996). Probe for B-subunit blots was produced using, as template, the 394 bp cDNA fragment of the V-ATPase B-subunit originally amplified with degenerate primers. Probe used for the strawberry control blots was produced using the strawberry DNA/pGEM-T easy vector construct for template. The construct was subjected to *Eco*R1 digestion prior to probe production and provided a template for oligonucleotide probes capable of recognizing synthetic RNA synthesized from the strawberry chitinase II clone.

Production of a recombinant protein for the V-ATPase B-subunit from A. franciscana

A region of the conserved central domain of the V-ATPase B-subunit from *Artemia franciscana*, corresponding to base pairs 728–1108, was amplified for in-frame insertion into a pET 30a(+) expression vector (Novagen, EMD Biosciences, San Diego, CA, USA) digested with *Eco*RI and *Xho*I restriction enzymes. The insert was sequenced directly from

the plasmid construct to confirm in-frame orientation of the B-subunit fragment insert with the T7 Lac Promoter and His Tag. The protocol for expression followed instructions in the pET System Manual (10th edition; Novagen) for pLysS host strain, BugBusters cell lysis, and denaturing inclusion body isolation. Protocol for Ni-NTA column chromatography followed that outlined for purification under denaturing conditions in the manual for His Bind kits (Novagen). Column eluate was concentrated using a Centricon centrifugal filter devise from Millipore (Billerica, MA, USA). Protein concentration was determined spectrophotometrically (A280).

Western blots

A. franciscana embryos were sampled after 0, 4 and 8 h of incubation at 22–23°C. Pre-emergence embryos were dechorionated immediately prior to homogenization, as previously described (Kwast and Hand, 1993). *Manduca sexta* midgut was removed and prepared for homogenization according to Harvey et al. (1990). Embryos were weighed and subjected to gentle homogenization in four volumes of buffer (300 mmol l^{-1} sucrose, 2 mmol l^{-1} EDTA, 50 mmol l^{-1} Hepes, pH 7.5) using 5–9 passes with a Teflon/smooth glass homogenizer from Thomas Scientific (Swedesboro, NJ, USA) and Glas-Col motor (Terre Haute, IN, USA) set at a maximum of 2000 r.p.m. Homogenates were subjected to differential centrifugation at 4°C to isolate subcellular fractions for electrophoresis (crude supernatant, 10 min at 1000 ***g***; mitochondrial pellet, 15 min at 9000 ***g***; heavy membrane pellet, 30 min at 48 000 ***g***; heavy microsomal vesicle pellet, 1 h at 100 000 ***g***; microsomal vesicle pellet and cytosolic supernatant, 1 h at 140 000 ***g***). Centrifugal forces were calculated for the maximum radius of JA 25.50 and Type 70.1Ti rotors (Beckman, Fullerton, CA, USA) used for centrifugation at $\leqslant$48 000 ***g*** and $\geqslant$100 000 ***g***, respectively. All centrifugation steps were performed in series using the supernatant of the previous spin, and samples were kept at 4°C throughout the procedure. Prior to western blotting, heavy and microsomal membrane preparations were subjected to osmotic shock by resuspending pellets in 35 ml and 8 ml, respectively, of a dilute buffer (10 mmol Tris-MOPS, pH 7.6). This procedure served to remove trapped soluble protein from vesicles and helped verify that dissociable V_1 subunits visualized in western blots were indeed associated with the membrane-spanning V_0 domain prior to electrophoresis. A second repetition of this procedure also served to reduce the non-specific background observed in western blots hybridized with the d-subunit antibody (Fig. 5C; lane W).

Samples were heat denatured for 45 s at 96°C in sample buffer (62.5 mmol l^{-1} Tris, pH 6.8, 2% SDS, 10% glycerol, 5% β-mercaptoethanol, 0.06 mg ml^{-1} bromophenol blue, final concentrations) and fractionated by discontinuous SDS–polyacrylamide gel electrophoresis using a Bio Rad (Hercules, CA, USA) Mini Protein 3 gel apparatus (100–140 V). Proteins were electrotransferred to nitrocellulose (0.2 μm Trans-Blot; Bio Rad) using a Bio Rad Mini Trans-Blot transfer cell (125 V for 1 h at <18°C). Blots were blocked with a casein solution (Vector Labs, Burlingame, MA, USA), incubated for 1 h with one of three polyclonal primary antibodies raised against the native V_1 complex (Huss, 2001), recombinant d-subunit of the V_0 domain (Reineke, 2002) or recombinant a-subunit of the V_0 domain (Reineke, 2002) from the V-ATPase of *Manduca sexta* larvae. An avidin/biotin blocking step was employed after primary antibody incubations to reduce nonspecific fluorescence. Blots were subsequently incubated for 30 min with the appropriate secondary antibodies (alkaline phosphatase conjugated or biotinylated) from Vector Labs. Fluorescent product for detection was created using a Vectastain ABC kit with DuoLux reagent (Vector Labs), and all blotting procedures were performed at 22–23°C.

Hatching studies

Prior to incubation in the treatment medium, embryos were rinsed briefly with 35‰ artificial seawater at 22°C. Unless otherwise stated, all embryos remained fully hydrated prior to incubation, and incubations were performed in a 9:1 mixture of artificial sea water (35‰) and 100% ethanol. All hatching incubations were conducted in 12-well plastic cell culture plates with 10–25 embryos per well. A single plate was used for each treatment, thus providing a total of 120–300 embryos per treatment group. In order to provide a high surface-to-volume ratio for gas exchange, only 0.5 ml of the incubation medium was placed into each well prior to the addition of embryos. To prevent evaporation of the treatment medium during lengthy incubations, a wet paper towel was placed over the top of each plate so that two ends of the towel were immersed in a distilled water bath. A cardboard box was then placed over the entire setup to limit photooxidation of the macrolide antibiotics used. Embryos were either allowed to develop undisturbed for 66–69 h before staging or were observed every 2 h over a 36 h period. All incubations were performed at 22°C.

Oligomycin (F-type ATPase inhibitor) was obtained from Sigma. The V-type ATPase inhibitor bafilomycin A_1 (also referred to as bafilomycin) was either obtained from AG Scientific (San Diego, CA, USA) or LC Laboratories (Woburn, MA, USA). Both oligomycin and bafilomycin were dissolved in 100% ethanol, and the stock solutions were stored at –20°C. The experimental concentrations of oligomycin and bafilomycin were varied and their effect on hatching success determined. Under the final conditions used (35‰ seawater + 10% ethanol), the limit of bafilomycin solubility was observed to be 6 μmol l^{-1}. Because bafilomycin is unstable in aqueous solution, the equivalent of 10 μmol l^{-1} bafilomycin was used to ensure a maximal effect during prolonged incubation.

Statistical analyses

All values are reported as means ± 1 S.E.M. Individual data points are given when $N<3$. Unless otherwise noted, means for mRNA abundance were compared among developmental time points using analysis of variance (ANOVA), while *post-hoc* multiple comparisons were made using Tukey's studentized

range (HSD) test. Inclusion of hour 0 values in comparisons among northern blot data summarized in Fig. 3B resulted in the violation of the assumption of homogeneity of variance, as determined by Levene's test for homogeneity (F=6.71, P=0.0033). Thus, comparisons between hour 0 and other time points were performed separately using the Kruskal–Wallis test, followed by the Nemenyi test (Zar, 1999). Statistical significance was set at $P \leqslant 0.05$ for all analyses.

Results

Molecular identification of B-subunit mRNA and phylogenetic comparisons

We identified expression of the V-ATPase B-subunit in encysted *Artemia franciscana* embryos by amplifying and sequencing a 394 bp cDNA fragment encoding a conserved central domain. The sequence for this cDNA was completed using a RACE protocol designed to amplify cDNA ends solely from full-length message having both an intact poly-A tail and a 7-methyl-guanosine cap. PCR reactions for both 3′ and 5′ RACE procedures produced single products, as observed by ethidium bromide staining of agarose gels (data not shown). Direct sequencing of PCR products yielded what appeared to be two overlapping sequences. To test whether this was caused by the presence of splice variants, the RACE products were cloned and sequenced directly from plasmid constructs. However, despite the sequencing of 20 clones, only a single cDNA sequence was observed for each end. The final assembled 1783 bp nucleotide sequence was submitted to GenBank (accession number, AY197611).

The putative start codon for the B-subunit of *A. franciscana* embryos is preceded by a 70-nucleotide 5′ untranslated region. The initiation sequence surrounding the start codon (AAAATGA) resembles that of a homologous subunit from the decapod crustacean *Carcinus maenas* (GenBank accession no., AAF08281; Weihrauch et al., 2001) but with an adenine at the #2 position instead of a cytidine. However, the *A. franciscana* initiation sequence differs greatly from that of the optimal Kozak initiation sequence (Kozak, 1991), with a complete absence of cytosine immediately upstream of the start codon and an adenosine in the #4 position. The stop codon begins at nucleotide 1565 and is followed by a relatively short 216-nucleotide 3′ untranslated region. Only a single adenosine and uridine-rich element (ARE) is present in this region, and polyadenylation begins at nucleotide 1772. The exact length of the poly-A tail is unknown, due to the use of a poly-T primer for reverse transcription. The complete transcript contains a single ORF, encoding 498 amino acids. The encoded protein has a calculated pI of 5.28, and its deduced molecular mass (55.5 kDa) closely matches values reported for B-subunit isoforms from other species (Filippova et al., 1998; Weihrauch et al., 2001). Definitive identification of the encoded protein was obtained *via* a BLAST search of the Conserved Domain Database (CCD; Marchler-Bauer et al., 2003), which revealed the presence of a highly conserved V-ATPase B-subunit NtpB domain, spanning amino acid positions 26–490 (Fig. 1).

Sequence alignments and phylogenetic analysis of the encoded protein were used to confirm the identity of the *A. franciscana* cDNA and infer potential subcellular localization patterns of the V-ATPase within encysted gastrula-stage embryos. The deduced *A. franciscana* B-subunit protein sequence demonstrates a slightly higher degree of amino acid identity with mammalian brain-type than kidney-type isoforms (Fig. 1), regardless of whether or not conserved amino acid substitutions are excluded as differences. This trend holds for both full-length (Fig. 1) and conserved NtpB domain (Fig. 2) alignments. Phylogenetic analysis of the conserved V-ATPase B-subunit NtpB domain, using deduced amino acid sequences, yielded two distinct groupings (Fig. 2). The first includes insects, crustaceans and the mammalian brain-type isoforms, while the second clade consists solely of mammalian kidney-type isoforms. The degree of support for the recovered clades was analyzed by bootstrapping with 1000 replicates. This analysis produced a significant bootstrap proportion of 76% for the clade grouping the *A. franciscana* protein with insects, crustacean and mammalian brain-type isoforms. Since V-ATPase with this B-subunit isoform is broadly localized and functionally diverse within these species (Futai et al., 2000), one might predict a broad functional repertoire and distribution within *A. franciscana* embryos as well. By contrast, the kidney-type isoforms of mammals are associated with V-ATPase that is primarily localized to the plasma membrane for the specific function of proton secretion. It is unclear as yet why the mammalian lineages maintain a strict conservation of the C- and N-terminal domains that is apparently not critical to its invertebrate counterpart. It is relevant to note, however, that inclusion of these domains did not affect the shape of the phylogenetic tree (data not shown) or the stated conclusions.

Analysis of V-ATPase mRNA expression during development

Northern blotting was performed to examine abundance of mRNA for the V-ATPase B-subunit throughout the early development of *A. franciscana* embryos. Two bands are visible in northern blots of total RNA samples hybridized with a probe produced from the *A. franciscana* B-subunit cDNA (Fig. 3A). The 3500 bp band is of much lower intensity than the 2250 bp band and decreases significantly during early development according to densitometric analysis, disappearing entirely after 24 h ($F_{4,14}$=15.94, P<0.0002). A similar analysis of the 2250 bp band suggests a decrease in the content of this message over the first 16 h of development, followed by an increase between 16 and 48 h. However, these changes in the 2250 bp band are not statistically significant ($F_{4,14}$=1.86, P=0.1938). Analysis of these data, in the absence of an internal control, is based on observations that both total RNA and ribosomal RNA remain relatively constant until 16–24 h of development at 30°C (Hofmann and Hand, 1992; Koller et al., 1987; McClean and Warner, 1971). The possibility remains, however, that expression levels beyond 16 h of development may be underestimated using this method, as total RNA has

been observed by Fisher (1986) to increase by 25% between hours 16 and 24 of aerobic development.

A second mRNA expression profile was produced in order to more rigorously test for differential expression inferred from the trends above for the 2250 bp transcript (see Materials and methods). In this experiment, synthetic plant RNA was used as an internal control for the examination of mRNA expression for the V-ATPase B-subunit. The profile produced with this method clearly demonstrates significant (H_4=14.942) differential expression of the 2250 bp band transcript during

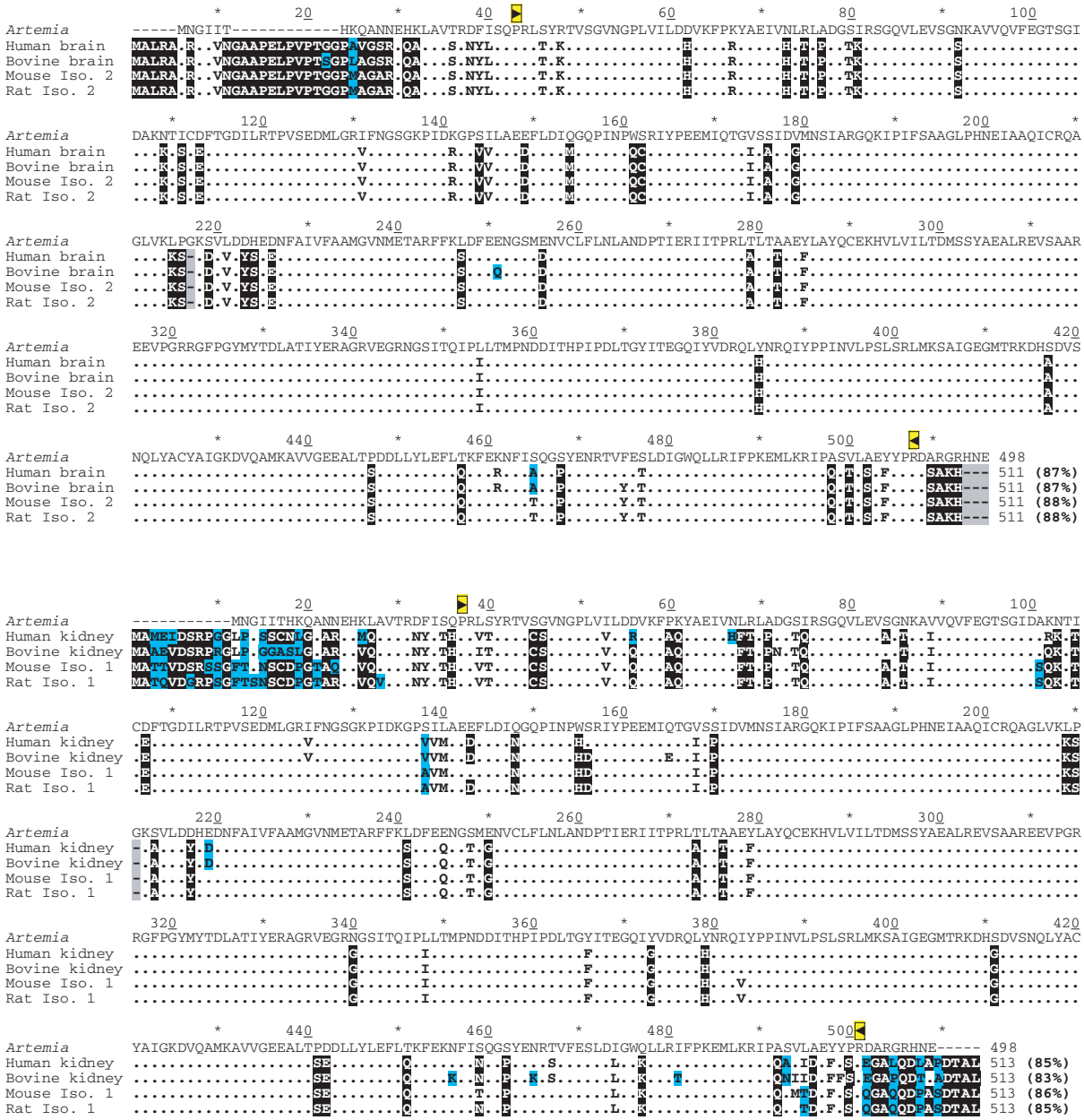

Fig.·1. (A) Alignment of the deduced amino acid sequence for the V-ATPase B-subunit from *Artemia franciscana* with mammalian brain-type (B2) isoforms (common name and GenBank accession numbers as follows: human, CAA44721; bovine, P31408; mouse, P50517; rat, NP_476561). (B) Alignment of the deduced amino acid sequence for the V-ATPase B-subunit from *A. franciscana* with mammalian kidney-type (B1) isoforms (human, NP_001683; bovine, P31407; mouse, NP_598918; rat, XP_232119). Sequence showing no differences between any of the species is represented by dots. White text on a black background represents mammalian sequence differing from *A. franciscana* but conserved among at least three of the four mammalian species (low variability). Black text on a blue background represents mammalian sequence differing both from *Artemia* and at least two mammalian sequences (high variability). Bold text on white background represents mammalian sequence with physiochemical properties similar to those of *Artemia* (potentially conserved). Gaps in the mammalian sequence are represented by a black dash on a grey background. The percent amino acid identity between aligned mammalian and *A. franciscana* sequence is enclosed in parentheses at the end of each sequence. Conserved NtpB domain used in phylogenetic analysis is bracketed by black and yellow arrow symbols above the *A. franciscana* sequence.

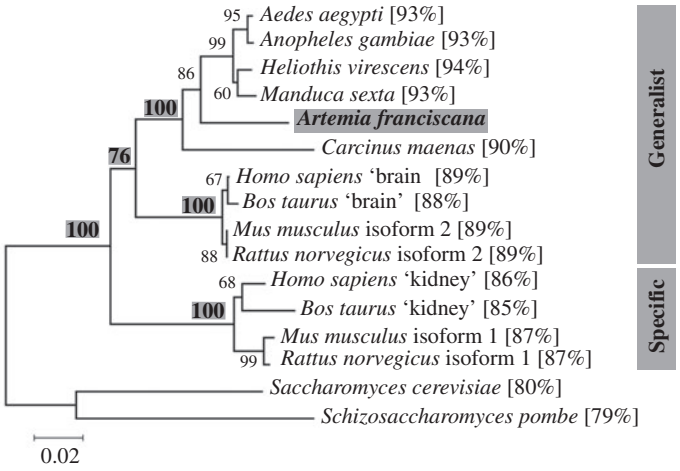

Fig. 2. Phylogenetic relationship of amino acid sequences for the NtpB domain from invertebrate, mammalian brain-type (B2), mammalian kidney-type (B1) and yeast V-ATPase B-subunit isoforms. GenBank accession numbers are listed here in descending order with respect to the cladogram, beginning with *A. aegypti* (AAD27666, XP_312029, P31410, P31401, AAP37188, AAF08281, CAA44721, P31408, P50517, NP_476561, NP_001683, P31407, NP_598918, XP_232119, P16140, P31411). Scale represents the proportion of amino acid difference between sequences. Bootstrap values from 1000 replicates are listed at each node. Sequences are placed into two groups, specific and generalist, based on the highlighted bootstrap values and general functional repertoire of the inclusive isoforms. Percent amino acid identity with the *A. franciscana* NtpB domain is recorded in parentheses after each species name.

the first 24 h of development (Fig. 3B). This B-subunit message drops by 47.0±2.8% during the first 12 h of aerobic development (Fig. 3B), at which point the embryo is in the process of emerging from its protective cyst wall (emergence stage 1; Fig. 3C). By 16 h of development, message levels have decreased by 59.4±3.3% relative to hour 0 (Fig. 3B), and the embryo is now enclosed only by a thin hatching membrane (emergence stage 2; Fig. 3C). By 24 h of development, the swimming nauplius predominates (Fig. 3C), and mRNA levels are no longer significantly different from 0 h. Thus, our second experiment confirms, with statistical significance, the trends seen for the 2250 bp transcript in the first experiment. Importantly, this confirmation comes with the use of two different RNA isolation procedures. The larger (⩾3500 bp) mRNA is also apparent in the northern blot of total RNA isolated by the RNeasy method but was too faint to allow confirmation of the trends seen in its expression from the first experiment (data not shown). It is noteworthy that a single B-subunit gene can produce multiple mRNA transcripts with differing sizes and developmental expression patterns. Work on the mosquito *Culex quinquefasciatus* shows the expression of two B-subunit transcripts in larvae (4.2 kb and 1.8 kb) but only one 3.0 kb transcript in pupae (Filippova et al., 1998). The northern blot results presented here suggest that a similar pattern may exist for *A. franciscana*. However, we were unable to identify more than one distinct cDNA in these embryos despite the sequencing of multiple clones.

Analysis of V-ATPase protein expression during development

To determine whether or not V-ATPase protein is expressed during early development, western blot analysis was performed on subcellular fractions isolated during the first 8 h of development. Unlike that reported for the decapod crustacean *C. maenas* (Weihrauch et al., 2001), *A. franciscana* blots hybridized with a monoclonal antibody raised against the B-subunit from yeast (Molecular Probes, Eugene, OR, USA) produced inconclusive results (data not shown). However, a polyclonal antibody raised against the native V_1 domain of the V-ATPase from *M. sexta* (Huss, 2001) did cross-react with four proteins present in heavy membrane, microsomal vesicle and soluble cytosolic fractions of *A. franciscana* lysates (Figs 4, 5A,B). These protein bands were identified as subunits A, B, E and G of the V-ATPase by comparison with immunoreactive proteins of similar size in lysates of *M. sexta* (Figs 4, 5B).

Further support for the identification of subunit B in *A. franciscana* lysates is provided by cross-reactivity of the V_1 antibody with a fragment of the *Artemia* B-subunit expressed *in vitro* (Fig. 4, lanes F1 and F2). This *in vitro*-expressed protein consists of 127 amino acids encoded by the *A. franciscana* B-subunit cDNA (amino acids 220–346), and 65 amino acids encoded by vector. The complete protein is 192 amino acids in length and has a calculated M_r of 21.4 kDa. This size closely matches that of the 25 kDa immunoreactive protein observed in northern blots of inclusion bodies isolated from the expression host (Fig. 4, lanes F1 and F2), thus confirming cross-reactivity of the V_1 antibody with the fusion protein. Recognition of vector sequence by the V_1 antibody is highly unlikely, since the antibody was raised against the native V_1 complex of *M. sexta*. In addition, it is unlikely that the antibody is detecting homologous F1 subunits from the mitochondrial ATP-synthase, since signals from mitochondrial preparations are very weak in comparison with post-mitochondrial fractions (Fig. 4, lane M). Control blots incubated with secondary antibody only demonstrate that the banding patterns present in mitochondrial preparations are largely nonspecific (Fig. 4, lane CM).

Identification of the 70 kDa A-subunit was confounded by the co-migration of a protein that gave a strong signal in all blots incubated with a biotinylated secondary antibody (Figs 4, 5A). For this reason, subunit A was visualized with a less-sensitive technique employing an alkaline phosphatase-conjugated secondary antibody (Fig. 5B). In these blots, expression of subunit A was detected in the microsomal fraction only (Fig. 5B, lane V^{140}). In blots incubated with a polyclonal antibody recognizing the d-subunit from *M. sexta*, three immunoreactive bands are visible (Fig. 5C,D). While difficult to discern from nonspecific background fluorescence, these bands appear only on blots incubated with the primary antibody recognizing *M. sexta* d-subunit and never on control blots. Two of these bands are present in heavy membrane

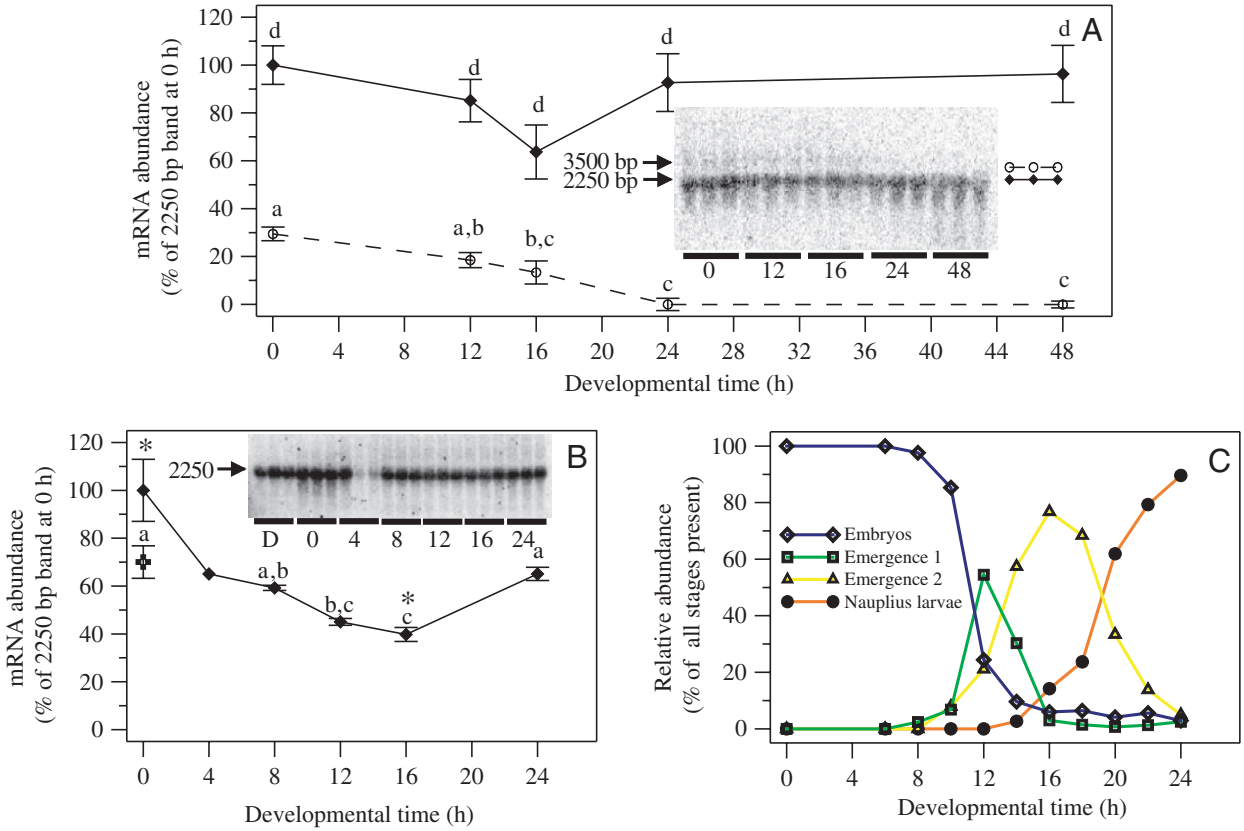

Fig. 3. Profile of mRNA expression for the V-ATPase B-subunit, as observed by northern blot analysis of total RNA isolated *via* (A) CsCl cushion or (B) RNeasy affinity spin column. Data for the 3500 bp message are plotted as circles with a broken line. Data for the 2250 bp message from post-diapause embryos are plotted as diamonds and a solid line, while that for diapause embryos are plotted as a cross. Two of the 4 h samples for plot B were excluded from analysis, as they formed insoluble precipitates during the drying step preceding suspension in gel loading buffer. For northern blots, values are expressed as means ± S.E.M. (N=3). Shared lowercase letters above error bars indicate that no significant difference exists between time points, as determined by Tukey's test. An asterisk denotes that a significant difference was found between two time points, as determined by the Nemenyi test. (C) Relative abundance of four *A. franciscana* developmental stages during incubation at 22–23°C. For each time point, a total of 332–631 individuals was counted, and the data were plotted as a percentage of the total.

preparations only (Fig. 5C; 44.6 and 43.6 kDa bands), while the third is present in both heavy membrane and microsomal vesicle preparations (Fig. 5C; 40.8 kDa band). A comparison with the *M. sexta* homologue suggests that the third, or smallest, of these bands is the d-subunit from the V-ATPase of *A. franciscana* (Fig. 5D). This band does not appear in the membrane-free cytosolic fraction.

Three immunoreactive bands (>105, 94 and 60 kDa) are also visible in blots of *Artemia* lysates incubated with a polyclonal antibody recognizing the a-subunit from *M. sexta* (Fig. 5E). The 94 kDa band was identified as subunit a based on size comparison with the *M. sexta* homologue. The >105 kDa band may be an aggregate with a second protein, as heat denaturing the sample for >1 min causes the 94 kDa band to disappear while the >105 kDa band increases in intensity for both *M. sexta* and *A. franciscana* samples (data not shown). The 60 kDa band is most likely to be a breakdown product of the 94 kDa a-subunit. All three of these bands appear in western blots of *M. sexta* membrane preparations (Fig. 5E, lane Ms).

Abundance of the membrane-bound d- and a-subunits from the V_0 domain does not change appreciably during the first 8 h of development (Fig. 5E). This finding stands in contrast to that for three of the soluble subunits of the V_1 domain (B, E and G), which show a small qualitative increase in expression within the heavy membrane fraction (Fig. 5A, lane H), but not in the larger cytosolic pool (Fig. 5A, lane S^{140}), over the same time period.

Effect of V-ATPase and ATP-synthase inhibitors on hatching success

Prior to inhibitor studies, tests were conducted to determine whether or not the ethanol used to solubilize inhibitors impacted hatching of embryos in varying salinities of artificial seawater. Ethanol had no effect on the hatchability of dechorionated embryos at concentrations of ⩽10% (Fig. 6). Concentrations in excess of 10% eventually caused bleaching of color and mortality, which indicates permeability of embryos to ethanol. It is of interest to note that the effect of ethanol and macrolide antibiotics on hatching success of dechorionated embryos was affected by the severity of the

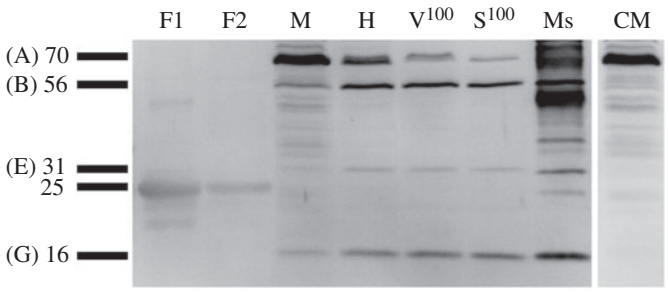

Fig. 4. Western blot analysis of *A. franciscana* B-subunit fusion protein (F1, 4 μg NtA column purified; F2, 7 μg solublized inclusion body), V-ATPase expression in subcellular fractions of encysted embryos (M, mitochondrial pellet; H, heavy membrane pellet; V^{100}, heavy microsomal vesicle pellet; S^{100}, supernatant of 100 000 ***g*** spin; 40 μg per lane) and a *Manduca sexta* positive control (Ms, heavy membrane pellet; 1 μg per lane). The blot on the left was incubated with primary antibody raised against the native V-ATPase V_1 complex purified from *Manduca sexta* midgut (Huss, 2001). All immunoreactive bands were identified by comparison with control blots incubated with secondary antibody only (blot not shown) and are listed in parentheses (together with their apparent M_r in kDa) to the left of the figure. The blot on the right (lane CM) is the control for mitochondrial lysates from *A. franciscana* (incubated with secondary antibody only) and is included to demonstrate that the banding in lane M is nonspecific.

dechorionation procedure. Both the age of the dechorionation solution and variation in the exposure to this solution influenced survivorship of subsequent treatments even though differences in embryos were not detected with light or scanning electron microscopy (J.A.C. and S.C.H., unpublished observations).

The permeability of encysted *A. franciscana* embryos to lipid-soluble inhibitors was determined by observing hatching success in varying concentrations of oligomycin, a macrolide antibiotic that specifically inhibits the F-type ATP-synthase of mitochondria. The ability of dechorionated embryos to develop beyond the encysted stage decreased as the concentration of oligomycin was increased. In contrast to the results presented below for bafilomycin, only an extremely small number of individuals developing beyond this stage ceased to develop during the subsequent E1 or E2 stages of emergence (Fig. 7A). Similar results were obtained if the dechorionated embryos were blotted dry prior to incubation, but the decrease in hatching success was more pronounced at lower concentrations of oligomycin (Fig. 7B), probably due to greater inhibitor uptake resulting from bulk flow of water during rehydration. By contrast, hatching of control embryos with an intact chorion was unaffected by oligomycin concentrations as high as 10 μmol l^{-1} (Fig. 7B).

Hatching studies obtained with bafilomycin, a specific inhibitor of the V-ATPase, indicated that embryos were also permeable to this plecomacrolide antibiotic, although the pattern of response differed from that seen with oligomycin. Specifically, inhibition of development was more pronounced

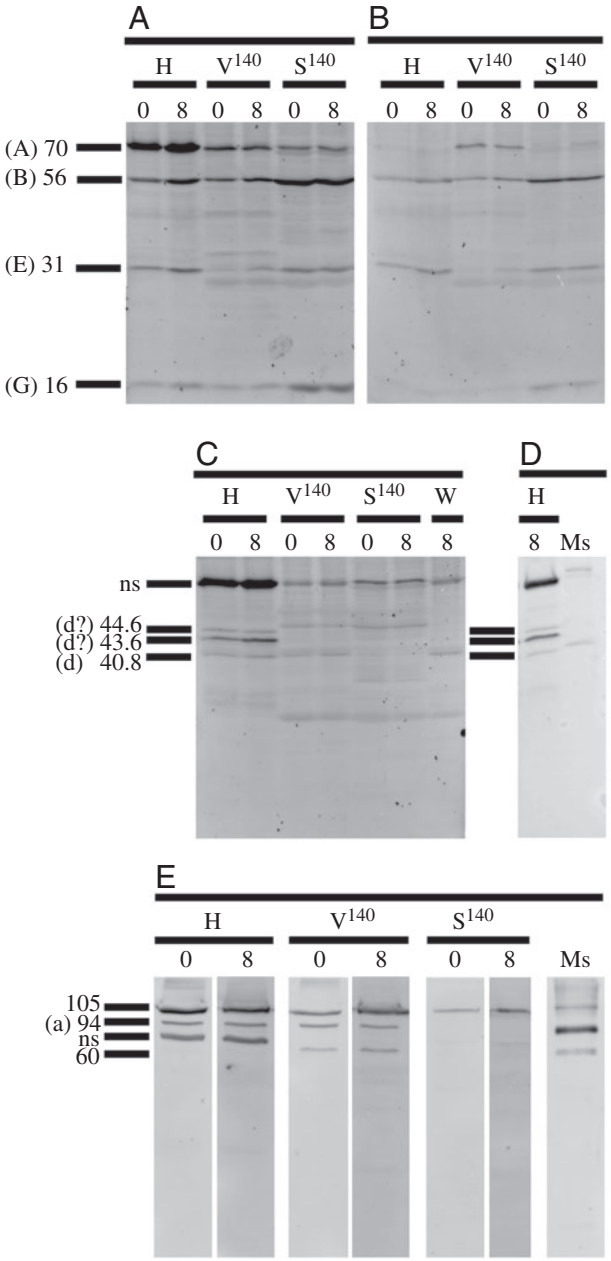

Fig. 5. Western blot analysis of V-ATPase expression in subcellular fractions of encysted embryos, employing three polyclonal antibodies raised against (A,B) the native V_1 complex, (C,D) recombinant d-subunit of the V_0 domain or (E) recombinant a-subunit of the V_0 domain from *Manduca sexta* larvae. A biotinylated secondary antibody was used for blots in A, C, D and E. An alkaline phosphatase-conjugated secondary antibody was used for blot in B to allow visualization of subunit A (70 kDa), which is obscured in biotinylated blots by a strong non-specific band (ns) visible in blots A, C, D and E. Subcellular fractions from 0 and 8 h of development were run side by side (H, heavy membrane; V^{140}, microsomal vesicles pelleted at 140 000 ***g***; S^{140}, post-ribosomal supernatant from 140 000 ***g*** spin; W, V^{140} pellet resuspended in buffer of low ionic strength and pelleted a second time; Ms, *Manduca sexta* heavy membrane preparation). All immunoreactive bands were identified by comparison with control blots incubated with secondary antibody only. Subunit designation (in parentheses) and apparent M_r (in kDa) for each band are listed to the left of each blot.

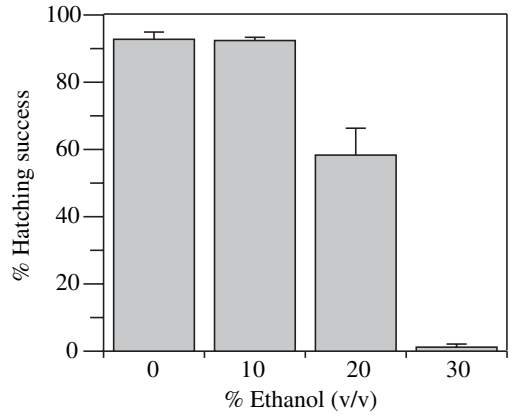

Fig. 6. Percentage of *A. franciscana* embryos developing to the swimming naupliar stage when incubated in 35‰ artificial seawater in the presence of 0, 10, 20 and 30% ethanol. Data are means ± S.E.M. (*N*=5).

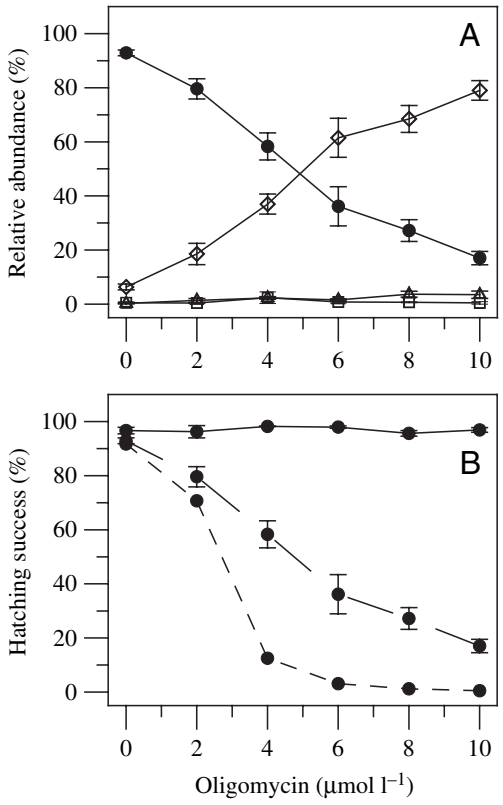

Fig. 7. Concentration dependence for inhibition of hatching in *A. franciscana* with oligomycin. (A) Simultaneous observation of the relative abundance of four developmental stages – dechorionated encysted embryos (open diamond), emergence 1 (open square), emergence 2 (open triangle) and nauplii (solid circle) – calculated as a percentage of all individuals present. (B) Percentage of individuals reaching the swimming naupliar stage under the following conditions: chorion intact (control; solid line), dechorionated (long dash line) and dechorionated followed by blotted dry before placement in incubation medium (short dash line). Data are means ± S.E.M. (*N*=3).

at lower concentrations for bafilomycin, and a larger percentage of embryos that began the emergence process arrested in the E1 or E2 stages with bafilomycin (Fig. 8A). The development of control embryos (chorion intact) was unaffected prior to the E2 stage, and then was inhibited only at concentrations of $\geqslant 6\ \mu mol\ l^{-1}$ (Fig. 8B). Periodic observation over 35 h demonstrated no noticeable effect of bafilomycin on the developmental rate of dechorionated embryos at inhibitor concentrations below $2\ \mu mol\ l^{-1}$ (Fig. 9A–C). Instead, as the concentration of bafilomycin was increased, a greater percentage of individuals stopped developing while in the encysted stage. The addition of $4\ \mu mol\ l^{-1}$ bafilomycin after 8 h of development depressed hatching (Fig. 9F), but not as much as when the inhibitor was present from hour 0 (Fig. 9E). Thus, bafilomycin is permeable to embryos during pre-emergence development. These results are the first to demonstrate a method for loading encysted embryos with lipid-soluble inhibitors and indicate a requirement for functional V-ATPase during pre-emergence development. Individuals that arrested during the process of emergence showed signs of emergence defects noted elsewhere (Trotman, 1991), suggesting that the V-ATPase is

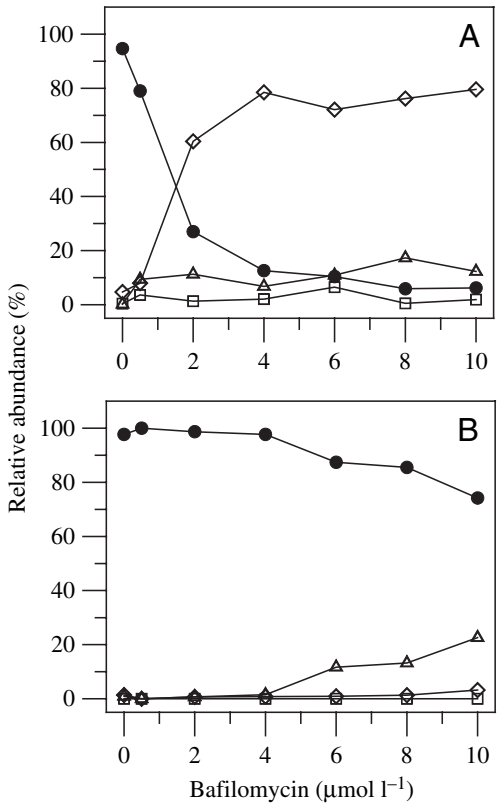

Fig. 8. Concentration dependence for inhibition of hatching in *A. franciscana* with bafilomycin. Observation of the relative abundance of four developmental stages – encysted embryos (open diamond), emergence 1 (open square), emergence 2 (open triangle) and nauplii (solid circle) – calculated as a percentage of all individuals present. Hatching studies were conducted using either (A) dechorionated embryos or (B) embryos with intact chorion.

also involved in the osmotic mechanism employed during emergence and hatching.

Discussion

The primary goals of the present study were to determine whether or not the V-ATPase proton pump occurs in *A. franciscana* embryos and, if so, to characterize this expression in the context of a potential role in anoxia signaling during pre-emergence development. We succeeded in demonstrating that (1) *bona fide* mRNA for subunit B of the V-ATPase is expressed during early development, (2) the deduced amino acid sequence of a B-subunit cDNA shows greater identity with the more broadly localized, and functionally diverse, homologues from other eukaryotes, (3) differential expression of B-subunit message occurs over developmental time, (4) at least six constituent subunits of the V-ATPase are expressed throughout encysted development, (5) subunits of both the V_1 and V_0 domains of the V-ATPase co-occur in both microsomal and heavy membrane preparations, (6) dechorionated embryos are permeable to the V-ATPase inhibitor bafilomycin and (7) inhibition of V-ATPase activity with bafilomycin interrupts embryonic development during the anoxia-tolerant stage. In the following discussion, we argue that these findings permit formulating an hypothesis whereby protons are first compartmentalized by the V-ATPase as part of normal gastrula-stage development and are subsequently released from these compartments into the cytoplasm upon exposure of the encysted embryo to anoxia. Such a release could facilitate the observed drop in intracellular pH, which has proven quantitatively inexplicable for more than two decades.

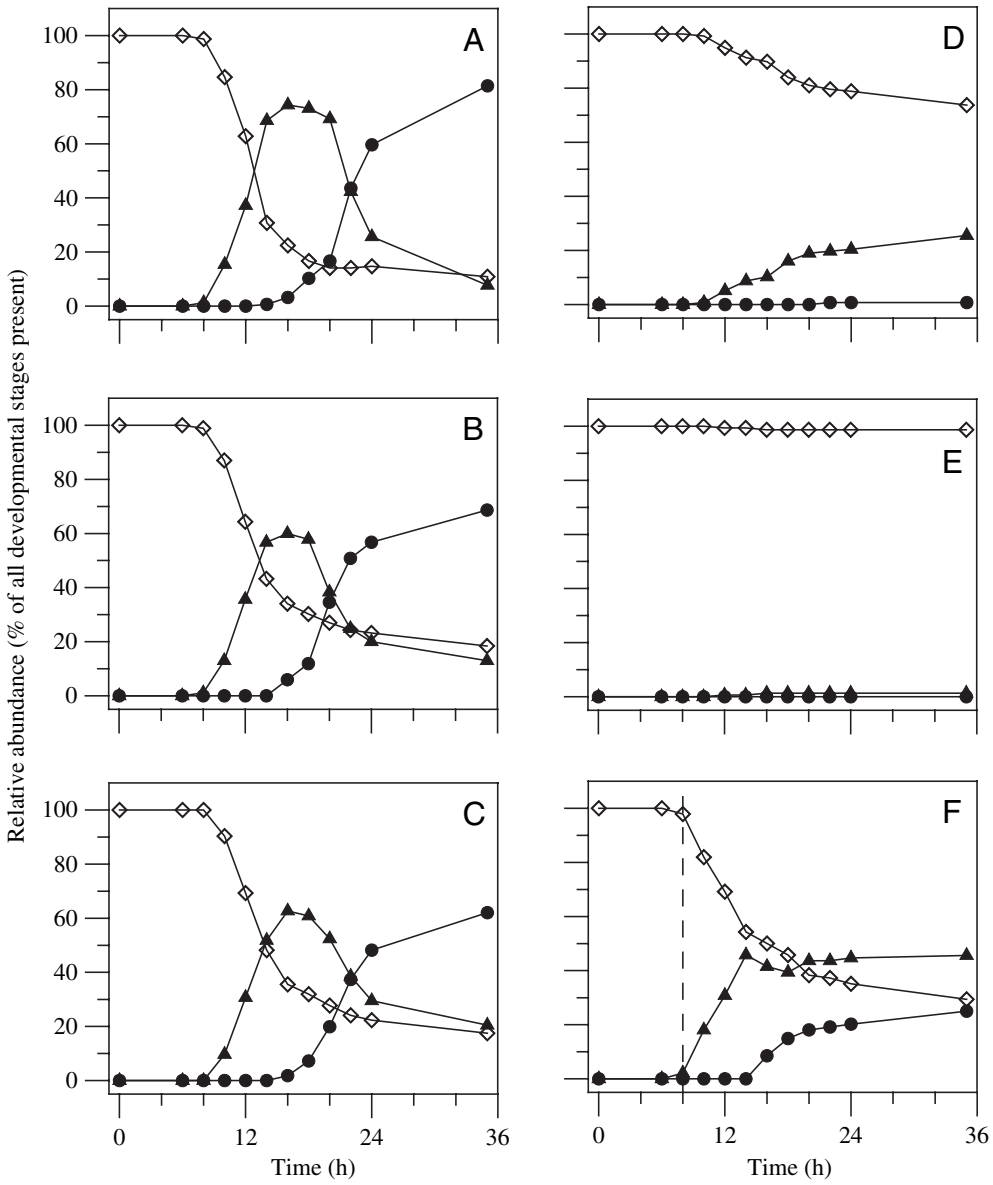

Fig. 9. Developmental time course of the relative abundance of three developmental stages – dechorionated encysted embryos (open diamond), emergence and emergence 2 stages combined (solid triangle) and nauplii (solid circle) – calculated as a percentage of all individuals present. Dechorionated embryos incubated in 35‰ Instant Ocean + 0.5% ethanol served as a control (A). Experimental treatments with 0.5 (B), 1.0 (C), 2.0 (D) and 4.0 μmol l^{-1} (E) bafilomycin in the presence of 0.5% ethanol began at hour 0. To determine whether or not embryos were permeable to bafilomycin prior to emergence, 4 μmol l^{-1} bafilomycin was added at hour 8 (F), as indicated with a broken line.

In order to better appreciate the role that acidic compartments might play in anoxia signaling, we examined the potential locations of such compartments within the anoxia-tolerant embryos by focusing on expression of the V-ATPase proton pump. All attempts to localize the V-ATPase using immunohistochemistry were unsuccessful. Thus, we employed a combination of sequence data analysis and western blotting to infer its subcellular distribution. Sequence alignments (Fig. 1) and phylogenetic analysis (Fig. 2) demonstrate that cDNA for the V-ATPase B-subunit of *A. franciscana* (Crustacea; Anostraca) groups with homologous B-subunit isoforms from invertebrates – specifically between the decapod crustacean *Carcinus maenas* and insects. A breakdown of this phylogenetic analysis produces two distinct

groupings: 'generalist' and 'specific', based on the subcellular localization and functional repertoire of the holoenzyme. The 'specific' grouping includes mammalian B-subunit isoforms known to be incorporated into V-ATPase employed specifically for proton secretion across the plasma membrane. By contrast, the 'generalist' grouping includes invertebrate and mammalian isoforms likely to be incorporated into V-ATPase present in both intracellular and plasma membranes for a diverse array of functions (Futai et al., 2000). Given that the *A. franciscana* isoform groups within the generalist clade, it is plausible that the V-ATPase of the anoxia-tolerant embryos is localized to both plasma and organellar membranes. Indeed, the western blot data presented here bolster this hypothesis, supporting the argument for a broadly localized distribution of V-ATPase within encysted embryos. The co-localization of V_1 domain subunits (B, E and G) with V_0 domain subunits (d and a) in both heavy and microsomal membrane preparations (Fig. 5) is consistent with the distribution of intact V-ATPase in both plasma and vesicular membranes during the earliest stages of encysted development. However, it should be noted that V-ATPase localization to the plasma membrane can be the result of participation in exocytosis or membrane energization, neither of which involve the establishment of a large proton chemical gradient (Harvey and Wieczorek, 1997). Thus V-ATPase-acidified compartments are likely to be intracellular.

An analysis of the V-ATPase expression data presented here in the context of recent literature strongly suggests a role for this enzyme in the establishment of intracellular proton stores in developing embryos. Wieczorek et al. (2000) noted that biosynthesis of V-ATPase subunits is tightly regulated in instances when the V-ATPase functions in a capacity other than the acidification of intracellular compartments. These authors point out that a molting-induced decrease in the activity of V-ATPase from *Manduca sexta* midgut parallels decreases in transcript levels for every subunit examined. However, for at least the first 8 h of development, such parallel changes are not apparent in *A. franciscana*, as the abundance of B-subunit mRNA during pre-emergence development (Fig. 3B) is not tightly linked to the level of the encoded protein incorporated into the holoenzyme (Fig. 5). Abundance of the 2250 bp B-subunit mRNA decreases consistently throughout the first 16 h of development (Fig. 3B), while western analyses suggest a modest increase in the incorporation of B-subunit protein in membrane-bound V-ATPase complexes. Based on these observations, one might suggest that acidification of intracellular compartments is the primary role for the V-ATPase of brine shrimp embryos. Indeed, published data regarding the development of *A. franciscana* embryos offer some support for this hypothesis. Increases in enzyme activities associated with transcription (Slegers, 1991) and in total protein labeling from pulse–chase experiments (Peterson et al., 1978) suggest an elevated demand for trafficking of newly synthesized proteins prior to emergence of the brine shrimp larva. In addition, both an embryonic cuticle and the first naupliar exoskeleton are synthesized by the epithelial cells during the process of emergence (Rosowski et al., 1997), suggesting the need for a very active exocytotic pathway between 8 and 24 h of development. Lysosomal activity has also been noted to be involved in the degradation of yolk platelets (Perona et al., 1988; Perona and Vallejo, 1989). Given that protein trafficking, yolk platelet degradation and exocytosis require V-ATPase-mediated acidification of lysosomes, transport vesicles and Golgi, it seems probable that the acidification of these intracellular compartments is a primary function of the brine shrimp enzyme during early development.

If proton chemical gradients are involved in anoxia signaling in brine shrimp embryos, a mechanism would be required to coordinate oxygen sensing with net proton flux from acidic compartments. Recently published work on vertebrate, insect and yeast V-ATPase suggests that the V-ATPase of brine shrimp embryos may be downregulated under anoxia by changes in ATP:ADP ratio and inorganic phosphate (P_i) concentration. For this reason, it is of interest that *A. franciscana* embryos deal with repeated and prolonged bouts of environmental anoxia by entering a reversible state of metabolic depression characterized, in part, by a reverse Pasteur effect. Under anoxia, these embryos rapidly shut down both catabolic and anabolic processes (Hand and Hardewig, 1996) and ultimately approach an ametabolic state (Warner and Clegg, 2001). Concomitant with this metabolic downregulation is a precipitous drop in adenylate status (Stocco et al., 1972). Over a 24 h period of anoxia, ATP levels decrease by 94.6±0.9% (Anchordoguy and Hand, 1994), with the majority of this decline occurring in the first few minutes. As a result, during the first 21 min of anoxia, the ATP:ADP ratio decreases from 7.6 to 0.92 (Anchordoguy and Hand, 1994) while [P_i] increases greatly (Rees et al., 1989). Importantly, recent catalytic analysis of V-ATPase from both insects and yeast demonstrates that even small reductions in the ATP:ADP ratio inactivate this proton pump (Huss and Wieczorek, 2003; Kettner et al., 2003), while work on vertebrates and yeast shows that both ADP (Kettner et al., 2003; Vasilyeva and Forgac, 1998) and P_i (David and Baron, 1994) have inhibitory effects on V-ATPase activity as well. If regulation by such biochemical variables occurs in *A. franciscana*, proton translocation by the V-ATPase would stop within minutes of anoxic exposure. Provided that all H^+ gradient dissipative paths are not concurrently downregulated, directional net H^+ flux would then dissipate existing gradients and acidify the surrounding cytoplasm. Interestingly, incubation of permeabilized mammalian cells in ATP-free medium resulted in a 0.7 pH unit alkalinization of the trans-Golgi network, which was fully reversed by the addition of exogenous ATP (Demaurex et al., 1998). These authors also demonstrate an alkalinization of Golgi during incubation with the V-ATPase inhibitor conconamycin. Similar effects were observed with bafilomycin incubation or ATP deprivation for yolk platelets of permeabilized *Xenopus* oocytes (Fagotto and Maxfield, 1994b). Taken together, these data suggest that inhibition of V-ATPase activity *via* a decrease in cellular ATP is enough to cause a net proton flux from organelles such as Golgi and yolk platelets to the cytosol.

Leakage of protons from intracellular compartments can significantly acidify the cytosolic space (Madshus et al., 1987). However, in any given cell, the effect of proton flux from these compartments would ultimately depend on their relative buffering capacities and size in relation to the surrounding cytoplasmic space. While we are unaware of any studies reporting these values in *Artemia* embryos, a large body of literature does describe such values for components of the protein synthetic, degradative, exocytotic and endocytotic pathways of other species (Ibarrola et al., 2000; Kelly et al., 1991; Rybak et al., 1997; Schoonderwoert and Martens, 2001; Van Dyke and Belcher, 1994; Wu et al., 2001). Based both on these data and published morphological studies on *Artemia* (Perona et al., 1988; Perona and Vallejo, 1989), one can estimate that Golgi, lysosomes and various transport vesicles constitute 2% of the intracellular volume in *Artemia* embryos and have a weighted average pH of 5.4 with a buffering capacity of 60 mmol H^+ l cytosol^{-1} pH unit^{-1} over the predicted range of compartment alkalinization under anoxia. It is also reasonable to include an estimate of the effect of proton release from membrane-bound yolk platelets in *Artemia*, the potential acidification of which has been discussed elsewhere (Busa et al., 1982; Fagotto, 1991). Because the yolk platelets of *Artemia* are most stable *in vitro* at a pH of 5.7 (Utterback and Hand, 1987), and an *in vivo* pH of 5.6 was observed for non-degrading yolk platelets in *Xenopus* oocytes (Fagotto and Maxfield, 1994a), it is plausible to assume a pH of 5.7 for the yolk platelets of *A. franciscana* embryos. We can also conservatively assume a buffering capacity of 60 mmol H^+ l cytosol^{-1} pH unit^{-1} given that 80% of embryonic protein is stored in the yolk platelets (Vallejo et al., 1981) and that yolk platelets of other species are known to have a high buffering capacity (Fagotto and Maxfield, 1994b). A two-dimensional analysis of electron micrographs generated by our lab (data not shown) suggests that approximately 15% of the embryonic space is occupied by yolk platelets. Using these data in conjunction with a general cytoplasmic buffering capacity of 18 mmol H^+ l cytosol^{-1} pH unit^{-1} published by Kwast et al. (1995), and assuming that intracellular compartments will not alkalinize above pH 6.4 under anoxia, one can estimate the contribution of protons from these compartments to be 50% of that required to explain the pH shift occurring during the first 20 min of anoxia†.

In summary, it seems improbable that a concentration gradient of protons could be maintained across lipid bilayers over years of anoxia in the face of an absence of available cellular energy for proton transport. We propose that, rather than undergoing a slow gradient dissipation spanning months or years, *A. franciscana* embryos experience an acute release of protons from acidic compartments, which is triggered by exposure to anoxia. Inactivation of H^+ pumping by the V-ATPase would be an essential step for such a process and may represent an adaptive trait critical to anoxia tolerance in this species. The data reported here demonstrate that this proton pump is differentially expressed during the period of encysted development characterized by anoxia tolerance, while inhibition of its activity with bafilomycin halts embryonic development. Together, these data demonstrate a critical need for proton pumping prior to the rapid growth phase accompanying emergence. Interestingly, the sharp decline in ATP:ADP ratio seen in *A. franciscana* under anoxia could inactivate the V-ATPase within minutes of exposure to anoxia. Subsequent dissipation of proton chemical gradients could help facilitate the observed cytoplasmic acidification required for quiescence. In the accompanying paper (Covi et al., 2005), we present ^{31}P-NMR experiments that directly test the ability of proton gradient dissipation to acidify the intracellular space.

This study was supported by National Science Foundation grant IBN9723746 and DARPA grant N00173-01-1-G011. We would like to thank Dr Helmut Wieczorek and Dr Markus Huss for assistance in selecting antibodies that recognize subunits of the V-ATPase from *A. franciscana*, for the generous donation of the three V-ATPase antibodies used in this study and for comments regarding this manuscript. We thank Leslie D. Lohmiller for technical assistance with bacterial culturing and statistical analysis using SAS software. We also thank Dr Brian Eads for useful comments regarding experimental design of northern blot assays, Dr Dirk Weihrauch for providing the degenerate primer sequences used to amplify B-subunit cDNA, Brad Marden and Jaimi Butler of INVE for assisting in the collection of diapause embryos, Dana Jones for assistance with sequencing, Daniel Ortiz-Barrientos for useful comments, and Dr Jim Belanger for graciously acquiring *Manduca sexta* larvae from the Arizona Research Labs Division of Neurobiology, University of Arizona.

References

Abreu, L. A., Valle, D., Manso, P. P., Facanha, A. R., Pelajo-Machado, M., Masuda, H., Masuda, A., Vaz, I., Jr, Lenzi, H., Oliveira, P. L. et al. (2004). Proteolytic activity of *Boophilus microplus* Yolk pro-Cathepsin D (BYC) is coincident with cortical acidification during embryogenesis. *Insect Biochem. Mol. Biol.* **34**, 443-449.

Anchordoguy, T. J. and Hand, S. C. (1994). Acute blockage of the ubiquitin-mediated proteolytic pathway during invertebrate quiescence. *Am. J. Physiol.* **267**, R895-R900.

Busa, W. B. and Nuccitelli, R. (1984). Metabolic regulation *via* intracellular pH. *Am. J. Physiol.* **246**, R409-R438.

Busa, W. B., Crowe, J. H. and Matson, G. B. (1982). Intracellular pH and the metabolic status of dormant and developing *Artemia* embryos. *Arch. Biochem. Biophys.* **216**, 711-718.

Carpenter, J. F. and Hand, S. C. (1986). Arrestment of carbohydrate metabolism during anaerobic dormancy and anaerobic acidosis in *Artemia* embryos: determination of pH-sensitive control points. *J. Comp. Physiol. B* **156**, 451-459.

†Calculations for the net release of protons sequestered in membrane-bound compartments, and its effect on pH_i: from yolk platelets, 0.15*v*/*v*×60 mmol l^{-1} β/*pH*×0.7 pH unit pa=6.3 mmol l^{-1} H^+; from Golgi, lysosomes and various transport vesicles, 0.02*v*/*v*×60 mmol l^{-1} β/*pH*×1.0 pH unit pa=1.2 mmol l^{-1} H^+; H^+ required for acidification/realkalinization of the cytoplasm across the pH range of 7.7 to 6.7, 0.83*v*/*v*×18 mmol l^{-1} β/*pH*×1.0 pH unit pa=15 mmol l^{-1} H^+. Thus, (1.2 mmol l^{-1}+6.3 mmol l^{-1})/15 mmol l^{-1}×100=50%. Abbreviations: *v*/*v*, the fraction of total embryonic volume; β/*pH*, the estimated average buffering capacity per pH unit over the relevant range of pH change; pa, the predicted total alkalinization of compartment under anoxia.

Clegg, J. S. (1974). Biochemical Adaptations Associated with Embryonic Dormancy of *Artemia-Salina*. *Trans. Am. Microsc. Soc.* **93**, 481-490.
Clegg, J. S. (2001). Cryptobiosis – a peculiar state of biological organization. *Comp. Biochem. Physiol. B Biochem. Mol. Biol.* **128**, 613-624.
Clegg, J. S., Jackson, S. A., Liang, P. and MacRae, T. H. (1995). Nuclear-cytoplasmic translocations of protein p26 during aerobic-anoxic transitions in embryos of *Artemia franciscana*. *Exp. Cell Res.* **219**, 1-7.
Conte, F. P., Droukas, P. C. and Ewing, R. D. (1977). Development of sodium regulation and *De Novo* synthesis of Na^+K-activated ATPase in larval brine shrimp, *Artemia salina*. *Exp. Zool.* **202**, 339-362.
Covi, J. A., Treleaven, W. D. and Hand, S. C. (2005). V-ATPase inhibition prevents recovery from anoxia in *Artemia franciscana* embryos: quiescence signaling through dissipation of proton gradients. *J. Exp. Biol.* **208**, 2799-2808.
Criel, G. R. J. (1991). Ontogeny of *Artemia*. In *Artemia Biology* (ed. R. A. Browne, P. Sorgeloos and C. N. A. Trotman), pp. 155-185. Boca Raton: CRC Press.
David, P. and Baron, R. (1994). The catalytic cycle of the vacuolar H^+-ATPase – comparison of proton transport in kidney-derived and osteoclast-derived vesicles. *J. Biol. Chem.* **269**, 30158-30163.
Demaurex, N., Furuya, W., D'Souza, S., Bonifacino, J. S. and Grinstein, S. (1998). Mechanism of acidification of the trans-Golgi network (TGN). In situ measurements of pH using retrieval of TGN38 and furin from the cell surface. *J. Biol. Chem.* **273**, 2044-2051.
Ewing, R. D. and Clegg, J. S. (1969). Lactate dehydrogenase activity and anaerobic metabolism during embryonic development in *Artemia salina*. *Comp. Biochem. Physiol.* **31**, 297-307.
Fagotto, F. (1991). Yolk degradation in tick eggs: III. Developmentally regulated acidification of the yolk spheres. *Dev. Growth Differ.* **33**, 57-66.
Fagotto, F. (1995). Regulation of yolk degradation, or how to make sleepy lysosomes. *J. Cell Sci.* **108**, 3645-3647.
Fagotto, F. and Maxfield, F. R. (1994a). Changes in yolk platelet pH during Xenopus laevis development correlate with yolk utilization. A quantitative confocal microscopy study. *J. Cell Sci.* **107**, 3325-3337.
Fagotto, F. and Maxfield, F. R. (1994b). Yolk platelets in Xenopus oocytes maintain an acidic internal pH which may be essential for sodium accumulation. *J. Cell Biol.* **125**, 1047-1056.
Fausto, A. M., Gambellini, G., Mazzini, M., Cecchettini, A., Masetti, M. and Giorgi, F. (2001). Yolk granules are differentially acidified during embryo development in the stick insect Carausius morosus. *Cell Tissue Res.* **305**, 433-443.
Filippova, M., Ross, L. S. and Gill, S. S. (1998). Cloning of the V-ATPase B subunit cDNA from *Culex quinquefasciatus* and expression of the B and C subunits in mosquitoes. *Insect Mol. Biol.* **7**, 223-232.
Fisher, J. A., Baxter-Lowe, L. A. and Hokin, L. E. (1986). Regulation of Na,K-ATPase biosynthesis in developing Artemia salina. *J. Biol. Chem.* **261**, 515-519.
Forgac, M. (1998). Structure, function and regulation of the vacuolar (H+)-ATPases. *FEBS Lett.* **440**, 258-263.
Forgac, M. (2000). Structure, mechanism and regulation of the clathrin-coated vesicle and yeast vacuolar H(+)-ATPases. *J. Exp. Biol.* **203**, 71-80.
Futai, M., Oka, T., Moriyama, Y. and Wada, Y. (1998). Diverse roles of single membrane organelles: factors establishing the acid lumenal pH. *J. Biochem. (Tokyo)* **124**, 259-267.
Futai, M., Oka, T., Sun-Wada, G., Moriyama, Y., Kanazawa, H. and Wada, Y. (2000). Luminal acidification of diverse organelles by V-ATPase in animal cells. *J. Exp. Biol.* **203**, 107-116.
Giorgi, F., Bradley, J. T. and Nordin, J. H. (1999). Differential vitellin polypeptide processing in insect embryos. *Micron* **30**, 579-596.
Grabe, M. and Oster, G. (2001). Regulation of organelle acidity. *J. Gen. Physiol.* **117**, 329-344.
Guppy, M. and Withers, P. (1999). Metabolic depression in animals: physiological perspectives and biochemical generalizations. *Biol. Rev.* **74**, 1-40.
Hand, S. C. (1997). Oxygen, pH_i and arrest of biosynthesis in brine shrimp embryos. *Acta Physiol. Scand.* **161**, 543-551.
Hand, S. C. (1998). Quiescence in *Artemia franciscana* embryos: reversible arrest of metabolism and gene expression at low oxygen levels. *J. Exp. Biol.* **201**, 1233-1242.
Hand, S. C. and Hardewig, I. (1996). Downregulation of cellular metabolism during environmental stress: mechanisms and implications. *Annu. Rev. Physiol.* **58**, 539-563.
Hand, S. C., Podrabsky, J. E., Eads, B. D. and van Breukelen, F. (2001). Interrupted development in aquatic organisms: Ecological context and physiological mechanisms. In *Environment and Animal Development. Genes, Life Histories and Plasticity* (ed. D. Atkinson and M. Thorndyke), pp. 219-234. Oxford, UK: BIOS Scientific Publishers Ltd.
Hardewig, I., Anchordoguy, T. J., Crawford, D. L. and Hand, S. C. (1996). Profiles of nuclear and mitochondrial encoded mRNAs in developing and quiescent embryos of *Artemia franciscana*. *Mol. Cell Biochem.* **158**, 139-147.
Harvey, W. R. and Wieczorek, H. (1997). Animal plasma membrane energization by chemiosmotic H^+ V-ATPases. *J. Exp. Biol.* **200**, 203-216.
Harvey, W. R., Crawford, D. N. and Spaeth, D. D. (1990). Isolation, voltage clamping, and flux measurements in lepidopteran midgut. *Methods Enzymol.* **192**, 599-608.
Hillis, D. M. and Bull, J. J. (1993). An empirical-test of bootstrapping as a method for assessing confidence in phylogenetic analysis. *Syst. Biol.* **42**, 182-192.
Hochachka, P. W. and Guppy, M. (1987). *Metabolic Arrest and the Control of Biological Time*. Cambridge, Mass.: Harvard University Press.
Hofmann, G. and Hand, S. (1992). Comparison of messenger RNA pools in active and dormant *Artemia franciscana* embryos: evidence for translational control. *J. Exp. Biol.* **164**, 103-116.
Huss, M. (2001). Struktur, Funktion und Regulation der Plasmamembran V-ATPase von *Manduca sexta*. In *des Fachbereichs Biologie/Chemie*, pp. 142. Osnabruck: Universitat Osnabruck.
Huss, M. and Wieczorek, H. (2003). The reversible dissociation of V-ATPase is influenced by nucleotides. *Comp. Biochem. Physiol.* **134**, 18.P2.
Ibarrola, I. I., Etxeberria, M., Iglesias, J. I., Urrutia, M. B. and Angulo, E. (2000). Acute and acclimated digestive responses of the cockle Cerastoderma edule (L.) to changes in the food quality and quantity. II. Enzymatic, cellular and tissular responses of the digestive gland. *J. Exp. Mar. Biol. Ecol.* **252**, 199-219.
Kawasaki-Nishi, S., Nishi, T. and Forgac, M. (2003). Proton translocation driven by ATP hydrolysis in V-ATPases. *FEBS Lett.* **545**, 76-85.
Kelly, C. W., Janecki, A., Steinberger, A. and Russell, L. D. (1991). Structural characteristics of immature rat Sertoli cells in vivo and in vitro. *Am. J. Anat.* **192**, 183-193.
Kettner, C., Obermeyer, G. and Bertl, A. (2003). Inhibition of the yeast V-type ATPase by cytosolic ADP. *FEBS Lett.* **535**, 119-124.
Khan, A. A. (2002). Characterization of chitinase activities, and cloning, analysis, and expression of genes encoding pathogenesis related proteins in strawberry. PhD thesis, Louisiana State University: Baton Rouge, LA, USA.
Koller, H. T., Frondorf, K. A., Maschner, P. D. and Vaughn, J. C. (1987). In vivo transcription from multiple spacer rRNA gene promoters during early development and evolution of the intergenic spacer in the brine shrimp *Artemia*. *Nucleic Acids Res.* **15**, 5391-5411.
Komazaki, S. and Hiruma, T. (1999). Degradation of yolk platelets in the early amphibian embryo is regulated by fusion with late endosomes. *Dev. Growth Differ.* **41**, 173-181.
Kozak, M. (1991). Structural features in eukaryotic mRNAs that modulate the initiation of translation. *J. Biol. Chem.* **266**, 19867-19870.
Kumar, S., Tamura, K. and Nei, M. (2004). MEGA3: Integrated software for molecular evolutionary genetics analysis and sequence alignment. *Brief Bioinform.* **5**, 150-163.
Kwast, K. E. and Hand, S. C. (1993). Regulatory features of protein synthesis in isolated mitochondria from *Artemia* embryos. *Am. J. Physiol.* **265**, R1238-R1246.
Kwast, K. E., Shapiro, J. I., Rees, B. B. and Hand, S. C. (1995). Oxidative phosphorylation and the realkalinization of intracellular pH during recovery from anoxia in *Artemia franciscana* embryos. *Biochim. Biophys. Acta* **1232**, 5-12.
Madshus, I. H., Tonnessen, T. I., Olsnes, S. and Sandvig, K. (1987). Effect of potassium depletion of Hep 2 cells on intracellular pH and on chloride uptake by anion antiport. *J. Cell. Physiol.* **131**, 6-13.
Marchler-Bauer, A., Anderson, J. B., DeWeese-Scott, C., Fedorova, N. D., Geer, L. Y., He, S., Hurwitz, D. I., Jackson, J. D., Jacobs, A. R., Lanczycki, C. J. et al. (2003). CDD: a curated Entrez database of conserved domain alignments. *Nucleic Acids Res.* **31**, 383-387.
McClean, D. K. and Warner, A. H. (1971). Aspects of nucleic acid metabolism during development of the brine shrimp *Artemia salina*. *Dev. Biol.* **24**, 88-105.
Nelson, N. and Harvey, W. R. (1999). Vacuolar and plasma membrane protonadenosinetriphosphatases. *Physiol. Rev.* **79**, 361-385.
Nelson, N., Perzov, N., Cohen, A., Hagai, K., Padler, V. and Nelson, H. (2000). The cellular biology of proton-motive force generation by V-ATPases. *J. Exp. Biol.* **203**, 89-95.

Nishi, T. and Forgac, M. (2002). The vacuolar (H+)-ATPases – nature's most versatile proton pumps. *Nat. Rev. Mol. Cell Biol.* **3**, 94-103.

Perona, R. and Vallejo, C. G. (1985). Acid-hydrolases during artemia development – a role in yolk degradation. *Comp. Biochem. Physiol. B Biochem. Mol. Biol.* **81**, 993-1000.

Perona, R. and Vallejo, C. G. (1989). Mechanisms of yolk degradation in *Artemia* – a morphological study. *Comp. Biochem. Physiol.* **94**, 231-242.

Perona, R., Bes, J. C. and Vallejo, C. G. (1988). Degradation of yolk in the brine shrimp Artemia. Biochemical and morphological studies on the involvement of the lysosomal system. *Biol. Cell* **63**, 361-366.

Peterson, G. L., Ewing, R. D. and Conte, F. P. (1978). Membrane differentiation and de Nova synthesis of the ($Na^+ + K^+$)-activated adenosine triphosphatase during development of *Artemia salina* nauplii. *Dev. Biol.* **67**, 90-98.

Rees, B. B., Ropson, I. J. and Hand, S. C. (1989). Kinetic properties of hexokinase under near-physiological conditions. Relation to metabolic arrest in Artemia embryos during anoxia. *J. Biol. Chem.* **264**, 15410-15417.

Reineke, S. (2002). Topologie und Regulation der *Manduca sexta* V-ATPase. PhD thesis, Universitat Osnabruck, Germany.

Reynolds, J. A. and Hand, S. C. (2004). Differences in isolated mitochondria are insufficient to account for respiratory depression during diapause in *Artemia franciscana* embryos. *Physiol. Biochem. Zool.* **77**, 366-377.

Rosowski, J. R., Belk, D., Gouthro, M. A. and Lee, K. W. (1997). Ultrastructure of the cyst shell and underlying membranes of the brine shrimp *Artemia franciscana* Kellogg (Anostraca) during postencystic development, emergence, and hatching. *J. Shellfish Res.* **16**, 233-249.

Rozen, S. and Skaletsky, H. (2000). Primer 3 on the WWW for general users and for biologist programmers. In *Bioinformatics Methods and Protocols: Methods in Molecular Biology* (ed. S. Krawetz and S. Misener), pp. 365-386. Totowa, NJ: Humana Press.

Rybak, S. L., Lanni, F. and Murphy, R. F. (1997). Theoretical considerations on the role of membrane potential in the regulation of endosomal pH. *Biophys. J.* **73**, 674-687.

Schoonderwoert, V. T. and Martens, G. J. (2001). Proton pumping in the secretory pathway. *J. Membr. Biol.* **182**, 159-169.

Slegers, H. (1991). Enzyme activities through development: a synthesis of the activity and control of the various enzymes as the embryo matures. In *Artemia Biology* (ed. R. A. Browne, P. Sorgeloos and C. N. A. Trotman), pp. 37-73. Boca Raton, FL: CRC Press.

Stocco, D. M., Beers, P. C. and Warner, A. H. (1972). Effect of anoxia on nucleotide metabolism in encysted embryos of the brine shrimp. *Dev. Biol.* **27**, 479-493.

Storey, K. B. and Storey, J. M. (1990). Metabolic rate depression and biochemical adaptation in anaerobiosis, hibernation and estivation. *Q. Rev. Biol.* **65**, 145-174.

Thompson, J., Gibson, T., Plewniak, F., Jeanmougin, F. and Higgins, D. (1997). The CLUSTAL_X windows interface: flexible strategies for multiple sequence alignment aided by quality analysis tools. *Nucl. Acids Res.* **25**, 4876-4882.

Trotman, C. N. A. (1991). Normality and abnormality in early development. In *Artemia Biology* (ed. R. A. Brown P. Sorgeloos and C. N. A. Trotman), pp. 75-92. Boca Raton: CRC Press.

Utterback, P. J. and Hand, S. C. (1987). Yolk platelet degradation in preemergence Artemia embryos: response to protons in vivo and in vitro. *Am. J. Physiol. Regul. Integr. Comp. Physiol.* **252**, R774-R781.

Vallejo, C. G., Perona, R., Garesse, R. and Marco, R. (1981). The stablility of the yolk granules of *Artemia*. an improved method for their isolation and study. *Cell Diff.* **10**, 343-356.

Van Dyke, R. W. and Belcher, J. D. (1994). Acidification of three types of liver endocytic vesicles: similarities and differences. *Am. J. Physiol. Cell Physiol.* **266**, C81-C94.

Vasilyeva, E. and Forgac, M. (1998). Interaction of the clathrin-coated vesicle V-ATPase with ADP and sodium azide. *J. Biol. Chem.* **273**, 23823-23829.

Warner, A. H. and Clegg, J. S. (2001). Diguanosine nucleotide metabolism and the survival of artemia embryos during years of continuous anoxia. *Eur. J. Biochem.* **268**, 1568-1576.

Warner, A. H. and Huang, F. L. (1979). Bioshynthesis of diguanosine nucleotides.2. mechanism of action of GTP-GTP guanylyltransferase on nucleotide-metabolism in brine shrimp embryos. *Can. J. Biochem.* **52**, 241-251.

Warner, A. H., Chu, P. P., Shaw, M. F. and Criel, G. (2002). Yolk platelets in artemia embryos: are they really storage sites of immature mitochondria? *Comp. Biochem. Physiol. B Biochem. Mol. Biol.* **132**, 491-503.

Weihrauch, D., Ziegler, A., Siebers, D. and Towle, D. W. (2001). Molecular characterization of V-type H(+)-ATPase (B-subunit) in gills of euryhaline crabs and its physiological role in osmoregulatory ion uptake. *J. Exp. Biol.* **204**, 25-37.

Wieczorek, H., Grber, G., Harvey, W. R., Huss, M., Merzendorfer, H. and Zeiske, W. (2000). Structure and regulation of insect plasma membrane H(+)V-ATPase. *J. Exp. Biol.* **203**, 127-135.

Willis, M. A. and Arbas, E. A. (1998). Variability in odor-modulated flight by moths. *J. Comp. Physiol. A* **182**, 191-202.

Wu, M. M., Grabe, M., Adams, S., Tsien, R. Y., Moore, H. P. and Machen, T. E. (2001). Mechanisms of pH regulation in the regulated secretory pathway. *J. Biol. Chem.* **276**, 33027-33035.

Zar, J. H. (1999). *Biostatistical Analysis*. New Jersey: Prentice-Hall.